Journal of Alloys and Compounds 509 (2011) 4117–4121

Contents lists available at ScienceDirect

Journal of Alloys and Compounds

journal homepage: www.elsevier.com/locate/jallcom

Conductivity and stability of cobalt pyrovanadate

Peter I. Cowin[a,b], Rong Lan[b], Christophe T.G. Petit[a,b], Lei Zhang[b], Shanwen Tao[a,b,*]

[a] Department of Chemical and Process Engineering, University of Strathclyde, Glasgow, G1 1XJ, UK
[b] Department of Chemistry, Heriot-Watt University, Edinburgh, EH14 4AS, UK

ARTICLE INFO

Article history:
Received 28 June 2010
Received in revised form
21 December 2010
Accepted 22 December 2010
Available online 31 December 2010

Keywords:
Conductivity
Cobalt pyrovanadate
Anode
Solid oxide fuel cell

ABSTRACT

Cobalt pyrovanadate was successfully synthesised by a solid state route and the conductivity in both oxidising and reducing environments was determined for the first time. Impedance measurements between 300 °C and 700 °C in air determined that $Co_2V_2O_7$ is an intrinsic semiconductor with activation energy of 1.16(3) eV. The conductivity in air reached a maximum of 4×10^{-4} S cm^{-1} at 700 °C. Semiconducting behaviour was also observed in 5% H_2/Ar, albeit with a much smaller activation energy of 0.04(4) eV. Between 300 °C and 700 °C the conductivity ranged from 2.45 S cm^{-1} to 2.68 S cm^{-1}, which is approaching the magnitude required for SOFC anode materials. Thermogravimetric analysis found a significant weight loss upon reduction of the compound. X-ray diffraction analysis, coupled with data from previous research, suggested compound degradation into $Co_{2-x}V_{1+x}O_4$, CoO and VO. The redox instability and the low conductivity lead us to the conclusion that cobalt pyrovanadate is unsuitable for utilisation as an anode material for SOFCs although the conductivity is reasonable in a reducing atmosphere.

1. Introduction

Development of novel anode materials for solid oxide fuel cells (SOFCs) is an essential step in the production of efficient intermediate temperature fuel cells. Extensive research has already been conducted in this area with some success [1–4], however the majority of anode materials consist of Ni-electrolyte cermets which still suffer from Ni agglomeration, fuel inflexibility and poor sulphur tolerance [5–8]. Additionally, many of these materials are developed for using at high temperature. Reduction of the temperature of SOFCs will allow for use of inexpensive metallic materials, will reduce start-up and shut down times and will reduce the interfacial reactions occurring between fuel cell components because the cross diffusion at the interfaces is less significant [9]. Further research is needed to identify compounds which contain all the appropriate properties necessary to produce an efficient anode material for use in intermediate temperature (500–700 °C) SOFCs.

Vanadium based compound have come under consideration as SOFC materials for both electrolyte and electrode application, as bismuth transition metal vanadates and rare earth vanadates respectively [10–12]. In general, vanadium containing compounds are of interest as anode materials due to their high catalytic activity [13] and the possibility of metallic-type conduction upon reduction [11,14].

$Co_2V_2O_7$ has been found to have a high catalytic activity for the selective oxidation of isobutene at 550 °C under anaerobic conditions [15], suggesting that the compound has labile lattice oxygen available for hydrocarbon oxidation. Cobalt pyrovanadate forms with the dichromate structure ($K_2Cr_2O_7$), space group $P2_1/c$, which consists of edge sharing CoO_6 octahedra and isolated pairs of VO_4 tetrahedra with a V-O-V angle of 117.5° [16]. According to the literature, $Co_2V_2O_7$ should be stable within SOFC operating ranges as the melting temperature is at either 830 °C [17] or 870 °C [18]. Partial reduction of these compounds should create the possibility of forming conductive, catalytically active compounds for use as SOFC anodes. Previous work on this compound has focused on the magnetic properties, catalytic efficiency or possible use in lithium batteries [15,19–21].

To the best of our knowledge, no research has been reported on the conductivity of cobalt pyrovanadate. Here we report on the conductivity and stability of $Co_2V_2O_7$ in both oxidising and reducing atmospheres. These properties can partially be used to determine the suitability of reduced $Co_2V_2O_7$ as an anode material for solid oxide fuel cells.

2. Experimental

2.1. Synthesis

$Co_2V_2O_7$ was synthesised by a conventional solid state method, according to previous work by Touaiher et al. [8]. Powders of $CoCO_3$ (99% metals basis, Alfa Aesar) and V_2O_5 (99.6+% metals basis, Sigma–Aldrich) were ground and fired sequentially at 150 °C, 300 °C and 450 °C for 24 h, 600 °C for 1 week and

* Corresponding author at: Department of Chemical and Process Engineering, University of Strathclyde, Glasgow, G1 1XJ, UK.
Tel.: +44 141 548 2361; fax: +44 141 548 2539.
E-mail address: shanwen.tao@strath.ac.uk (S.W. Tao).

0925-8388/$ – see front matter © 2010 Elsevier B.V. All rights reserved.
doi:10.1016/j.jallcom.2010.12.166

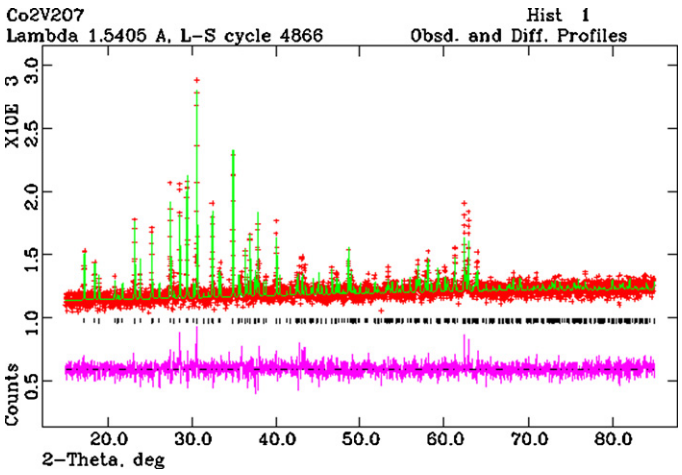

Fig. 1. Rietveld refinement of $Co_2V_2O_7$ using GSAS.

700 °C for 24 h with an intermediate grinding step in between each firing. Pellets (⌀ ≈ 13 mm × 2 mm) were uniaxially pressed at 221 MPa and sintered in air at 700 °C for 12 h.

2.2. Analytical procedures

Phase purity and crystal parameters of the samples were examined by X-ray diffraction (XRD) analysis using a Bruker D8 Advance diffractometer (Cu Kα1 radiation, λ = 1.5405 Å). GSAS [22] software was used to perform a least squares refinement of the lattice parameters of all the samples. XRD analysis was performed post-sintering and post-conductivity measurements in both air and 5% H_2/Ar, without re-oxidation.

The densities of the pellets were determined from the measured mass and volume prior to conductivity measurements. Theoretical densities were calculated using experimental lattice parameters and the chemical formula $Co_2V_2O_7$. The relative densities were calculated from the actual and theoretical density values. The average relative densities of the pellets were determined to be 73%.

Thermal analysis was conducted using a Stanton Redcroft STA 1500 Thermal Analyser on heating from room temperature to 700 °C and on cooling from 700 °C to room temperature in air, with a heating/cooling rate of 5 °C min^{-1}, and in 5% H_2/Ar, again with a heating/cooling rate of 5 ° min^{-1}, and with a flow rate of 5% H_2/Ar of 20 mL min^{-1}. The sample was mounted in a platinum crucible with Pt-Rh used as a reference material.

2.3. Conductivity testing

The pellets (⌀ ≈ 13 mm × 2 mm) were coated on opposing sides using platinum paste and fired at 700 °C for 12 h. The conductivity of the samples was measured in the range 300–700 °C. Measurements in air were conducted using a psudeo-4-probe A.C. method using a Solartron Analytical 1287 electrochemical interface coupled with a Solartron Analytical 1250 frequency response analyser controlled by ZPlot software over the frequency range 65 kHz to 100 mHz. Measurements in dry 5% H_2/Ar, dried by passing the gas through 98% H_2SO_4, were conducted using a D.C. method using a Solartron Analytical 1287 electrochemical interface controlled by Scribner Associates Inc CorrWare software with a constant current of 0.001 A, after reduction in the same atmosphere at 600 °C for 275 min.

3. Results and discussion

3.1. Structure

X-ray diffraction analysis, alongside Rietveld refinement (shown in Fig. 1), indicates that single phase $Co_2V_2O_7$ was successfully synthesised. The refinement used a single phase set-up with $Co_2V_2O_7$ modelled using a $P2_1/c$ space group, $a = 6.594(2)$ Å, $b = 8.380(1)$ Å, $c = 9.470(9)$ Å and $\beta = 100.17(3)°$ [23]. The refinement gave χ^2, wR_p and R_p values of 1.479, 3.47% and 2.68%, respectively, indicating a good fit to the experimental data and confirmed the formation of $Co_2V_2O_7$. The lattice parameters are similar to those found previously [14] with the lattice parameters not differing by more than 0.01 Å or 0.5°; $a = 6.593(8)$ Å, $b = 8.37(1)$ Å, $c = 9.48(1)$ Å and $\beta = 100.22(2)°$.

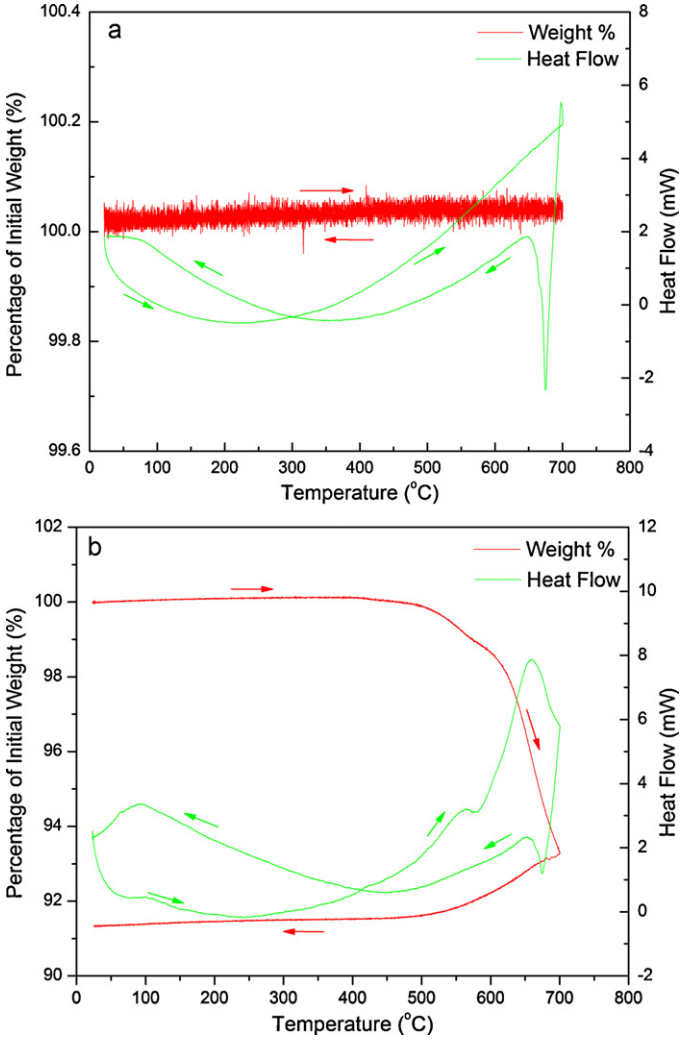

Fig. 2. TG–DSC analysis of the $Co_2V_2O_7$ sample in air (a) and 5% H_2/Ar (b). Ramp rate 5 °C/min, 5% H_2/Ar flow rate 20 ml/min.

3.2. Thermal analysis

Thermal stability was analysed using thermogravimetric analysis (TGA) and differential scanning calorimetry (DSC) curves. Fig. 2 shows the TGA and DSC curves of $Co_2V_2O_7$ from room temperature to 700 °C in both air and dry 5% H_2/Ar.

The TGA of $Co_2V_2O_7$ in air exhibits no significant changes in compound weight. The DSC trace of $Co_2V_2O_7$ in air shows no obvious phase transitions, as would be expected from previous research [9,10]. The deviation of the DSC curve observed between 700 °C and 650 °C on the DSC trace is due to the lag of the instrument on changing from heating to cooling.

In 5% H_2/Ar the TGA trace of $Co_2V_2O_7$ shows no change up to ~420 °C, at which weight loss begins to occur. A small peak can be observed on the DSC trace at 575 °C which corresponds to the kink in the TGA trace, suggesting that this is the result of non-linear reduction. At 500 °C significant weight loss occurs, which corresponds with an increase in heat flow on the DSC trace suggesting that the weight loss is exothermic. Lag is again noted on the transition from heating to cooling on the DSC trace. The total weight loss

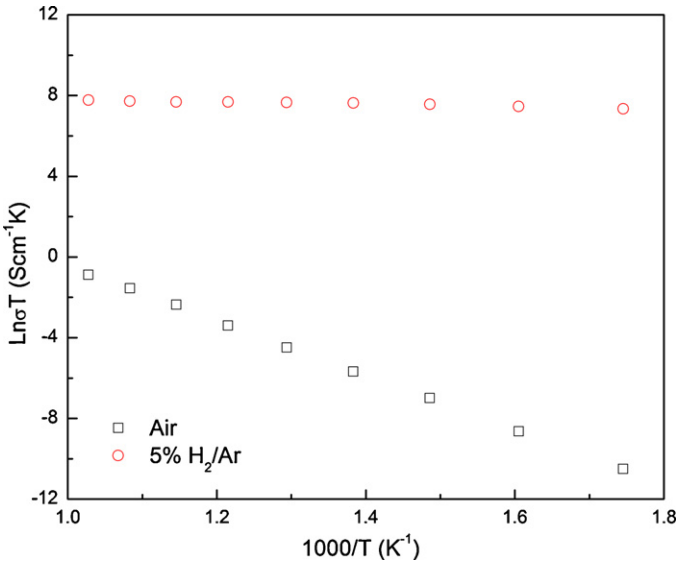

Fig. 3. Total conductivity of $Co_2V_2O_7$ in air and dry 5% H_2/Ar as a function of temperature plotted in Arrhenius form.

after reduction is 8.77% and is likely to be due to the loss of oxygen from compound decomposition.

3.3. Conductivity and redox stability

The conductivity of the sample was measured between 300 °C and 700 °C in both air and 5% H_2/Ar. Fig. 3 exhibits a single conduction mechanism over the measured temperature range in air. The conductivity ranges from 5×10^{-8} S cm^{-1} at 300 °C and 4×10^{-4} S cm^{-1} at 700 °C with calculated activation energy for conduction of 1.16(3) eV. Typical impedance spectra demonstrating the shifts in the observable phenomena over the frequency range are presented in Fig. 4. Both the bulk and grain boundary conductivities are evident in Fig. 4a, identified by the characteristic capacitance of each electrochemical process [24]. As the temperature increases these features shift to higher frequencies and thus the electrodic resistance becomes observable, as shown in Fig. 4b. This shift prevents accurate separation of the bulk and grain boundary conductivities throughout the measured temperature range, thus total conductivity, a combination of bulk conductivity and grain boundary conductivity, is used.

In $Co_2V_2O_7$, cobalt is found in edge sharing octahedra with a cobalt-cobalt distance of ~3 Å [8], thus the likely percolation pathway is through electron hopping between cobalt d-orbitals. Additionally, the isolated nature of the vanadium tetrahedra and the structural change of vanadium upon reduction intimates that conduction between vanadium d-orbitals is unlikely to be the dominant pathway for conduction.

In 5% H_2/Ar the conductivity exhibits a single conduction mechanism with a calculated activation energy of 0.04(4) eV. The conductivity shows a significant increase upon reduction, as evidenced in Fig. 5. The sample is almost fully reduced after exposure to 5% H_2/Ar at 700 °C for 1 h. Conductivity in 5% H_2/Ar between 300 °C and 700 °C ranges from 2.68 S cm^{-1} to 2.45 S cm^{-1}. The significant change in conductivity, in conjunction with the weight change upon reduction from the thermogravimetry data, implies that the compound degrades upon reduction.

The X-ray diffraction data of the reduced sample, Fig. 6, displays no evidence of $Co_2V_2O_7$, which, in conjunction with the TGA/DSC data, leads to the conclusion that $Co_2V_2O_7$ is not redox stable. The compound appears to decompose into Co_2VO_4 (JCPDS num-

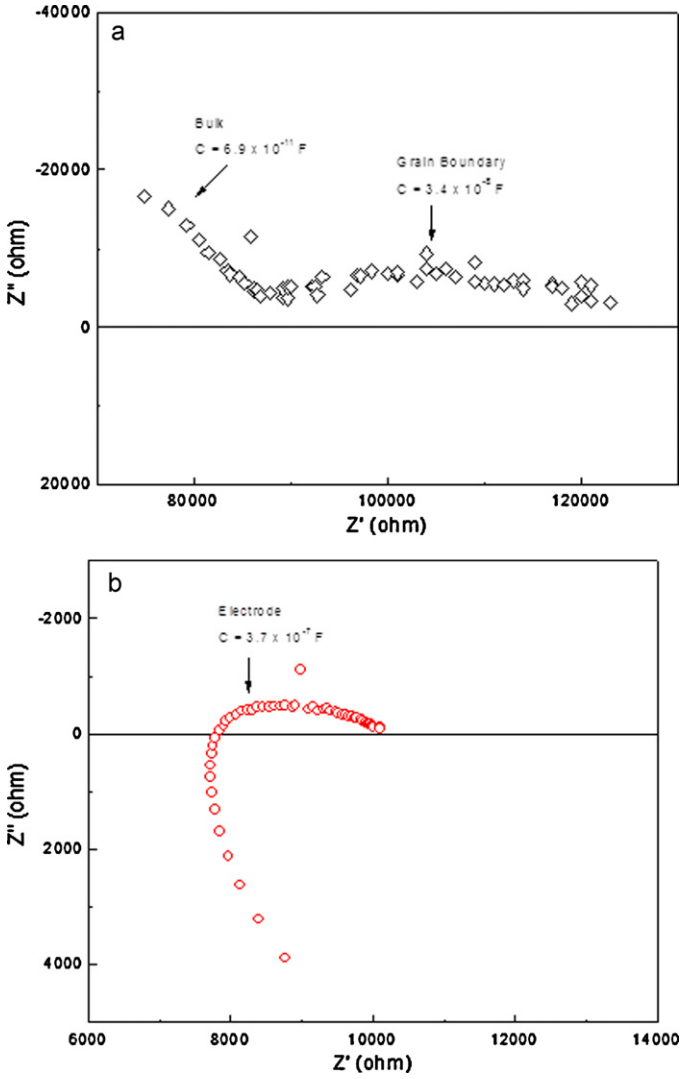

Fig. 4. Complex impedance plots and equivalent circuit diagrams for $Co_2V_2O_7$ in air at 400 °C (a) and 550 °C (b).

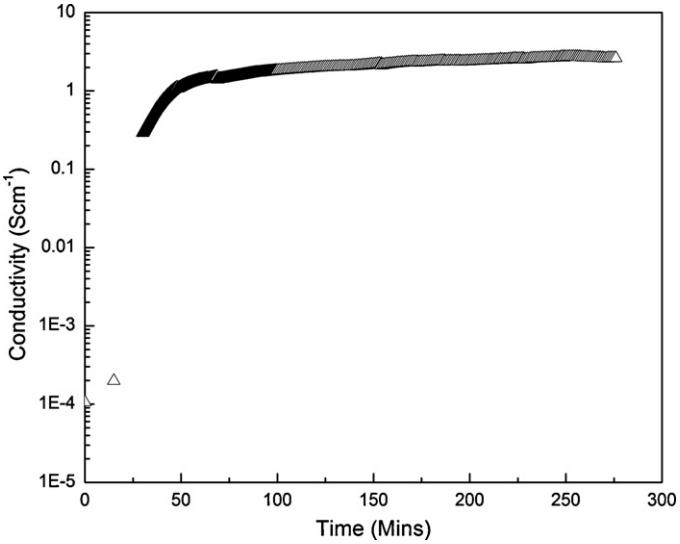

Fig. 5. Stabilisation of the conductivity of $Co_2V_2O_7$ in dry 5% H_2/Ar at 600 °C using both AC and DC techniques.

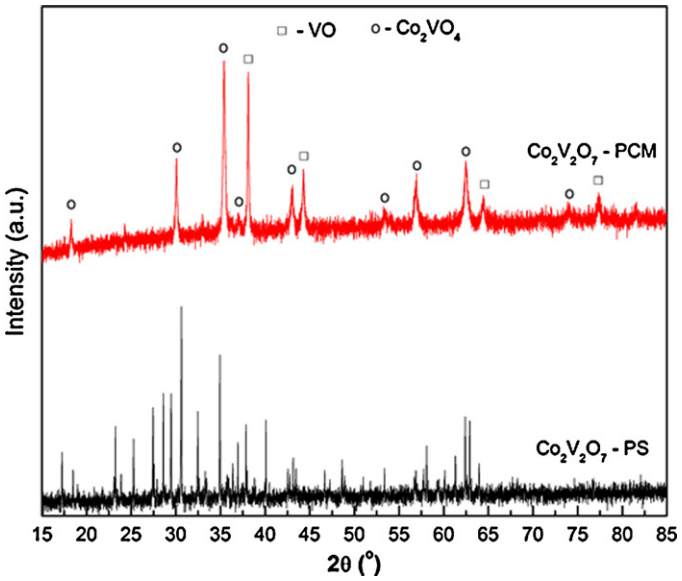

Fig. 6. X-ray diffraction pattern of $Co_2V_2O_7$ post sintering (PS) and after reducing in 5% H_2/Ar at 700 °C for 12 h.

ber 01-073-1633) and VO (JCPDS number 03-065-2896) through the degradation pathway below:

$$Co_2V_2O_7 \xrightarrow{600\,^\circ C,\ 5\%H_2/Ar} Co_2VO_4 + VO + 2H_2O \quad (1)$$

Thermogravimetric analysis, Fig. 2, revealed a weight loss of 8.77% upon reduction of the compound. This correlates well with the theoretical weight loss from the decomposition route given in Eq. (1), 9.64%. The difference between the values is likely due to incomplete reduction of the compound during thermogravimetric analysis.

Co_2VO_4 is cubic, space group $Fd\bar{3}m$, with vanadium and cobalt randomly distributed in 12-coordinate sites and edge-sharing MO_6 octahedra [25]. From geometric considerations, this compound is likely to have conduction through the mixed transition metal octahedra. Cobalt in this compound is found as Co^{2+}, which has the electronic structure $3d^7$, $t_{2g}{}^5$ $e_g{}^2$, Due to electron-electron repulsion, conduction through cobalt octahedra is likely to have higher activation energy for conduction that through vanadium, found as V^{4+}, with the electronic configuration $3d^1$, $t_{2g}{}^1$ $e_g{}^0$.

Previous research indicates that the activation energy observed for this compound, 0.04 eV, correlates well to that found by Rogers et al. in 1963 for CoV_2O_4, 0.07 eV, while a much higher activation energy was observed for Co_2VO_4, 0.37 eV [26]. Both Co_2VO_4 and CoV_2O_4 form with the spinel structure, although with differing distributions of cobalt and vanadium cations and, therefore, have similar X-ray diffraction patterns. No information is available on the thermal properties of either of these compounds, however as the DSC curve does not demonstrate any significant peaks on cooling, no differentiation between these compounds would have been available using this data. The activation energy would suggest that the decomposition route in Eq. (2) is more credible, despite the evidence to the contrary from XRD analysis.

$$Co_2V_2O_7 \xrightarrow{600\,^\circ C,\ 5\%H_2/Ar} CoV_2O_4 + CoO + 2H_2O \quad (2)$$

It is also possible that non-stoichiometric phases were formed during decomposition, which would proceed through the route suggested in Eq. (3).

$$Co_2V_2O_7 \xrightarrow{600\,^\circ C,\ 5\%H_2/Ar} Co_{2-x}V_{1+x}O_4 + xCoO + (1-x)VO + 2H_2O \quad (3)$$

Considering that vanadium monoxide was formed upon reduction, the decomposition route proposed in Eq. (2) is less probable than that proposed in Eq. (3). Taking into account the impurity of the sample, the magnitude of the conductivity for a pure, dense sample of CoV_2O_4 should be significantly higher than the observed conductivity. Despite the possible increased conductivity, research into alternative transition metal spinels found significant redox instability [27]. Due to the high probability of redox instability, this compound is unlikely to be a suitable candidate for an anode material for solid oxide fuel cells.

4. Conclusions

Cobalt pyrovanadate was successfully synthesised using a solid state synthesis techniques. Impedance measurements between 300 °C and 700 °C in air determined that $Co_2V_2O_7$ is an intrinsic semiconductor with a band gap of 1.16(3) eV. The conductivity of the sample in 5% H_2/Ar also exhibits semiconductor behaviour, albeit with a much smaller activation of 0.04(4) eV. The conductivity in air reached a maximum of 4×10^{-4} S cm^{-1} at 700 °C. In 5% H_2/Ar, albeit with a much smaller activation energy of 0.04(4) eV, the conductivity ranged from 2.45 S cm^{-1} to 2.68 S cm^{-1}, which is approaching the magnitude required for SOFC anode materials.

Thermogravimetric analysis found a significant weight loss upon reduction of the compound and X-ray diffraction analysis indicated compound degradation into $Co_{2-x}V_{1+x}O_4$, CoO and VO. The redox instability and the low conductivity lead us to the conclusion that cobalt pyrovanadate is unsuitable for utilisation as an anode material for SOFCs although the conductivity is reasonable in a reducing atmosphere. Conductivity measurements on a pure sample of CoV_2O_4 should result in significant increases in the observed magnitude of the conductivity.

Acknowledgements

We would like to thank EPSRC and the ScotChem SPIRIT scheme for funding. We would also like to thank Marian Millar for her aid with X-ray diffraction data collection.

References

[1] S.W. Tao, J.T.S. Irvine, Nat. Mater. 2 (2003) 320–323.
[2] J.C. Ruiz-Morales, J. Canales-Vásquez, C. Savaniu, D. Marrero-López, W. Zhou, J.T.S. Irvine, Nature 439 (2006) 568–571.
[3] Y.-H. Huang, R.I. Dass, Z.-L. Xing, J.B. Goodenough, Science 312 (2006) 254–257.
[4] S.W. Tao, J.T.S. Irvine, Solid State Ionics 179 (2008) 725–731.
[5] C.M. Grgicak, R.G. Green, J.B. Giorgi, J. Power Sources 179 (2008) 317–328.
[6] D. Simwonis, F. Tietz, D. Stöver, Solid State Ionics 132 (2000) 241–251.
[7] K.F. Chen, Z. Lu, X.J. Chen, N. Ai, X.Q. Huang, B. Wei, J.Y. Hu, W.H. Su, J. Alloys Compd. 454 (2008) 447–453.
[8] T.S. Li, W.G. Wang, H. Miao, T. Chen, C. Xu, J. Alloys Compd. 495 (2010) 138–143.
[9] J.P.P. Huijsmans, F.P.F. van Berkel, G.M. Christie, J. Power Sources 71 (1998) 107–110.
[10] F. Abraham, J.C. Boivin, G. Mairesse, G. Norogrocki, Solid State Ionics 40–41 (1990) 934–937.
[11] Z. Cheng, S. Zha, L. Aguilar, M. Liu, Solid State Ionics 176 (2005) 1921–1928.
[12] M.M. Cooper, K. Channa, R. De Silva, D.J. Bayless, J. Electrochem. Soc. 157 (2010) B1713–B1718.
[13] Z. Xu, J. Luo, K.T. Chuang, ECS Trans. 11 (2008) 1–17.
[14] C.T.G. Petit, R. Lan, P.I. Cowin, J.T.S. Irvine, S.W. Tao, J. Mater. Chem. 21 (2010) 525–531.
[15] Y. Takita, S. Hikazudani, K. Soda, K. Nagaoka, J. Mol. Catal. A: Chem. 280 (2008) 164–172.
[16] M. Touaiher, K. Rissouli, K. Benkhouja, M. Taibi, J. Aride, A. Boukhari, B. Heulin, Mater. Chem. Phys. 85 (2004) 41–46.
[17] G.M. Clark, A.N. Pick, J. Therm. Anal. 7 (1975) 289–300.
[18] M. Kurzawa, M. Bosacka, J. Therm. Anal. Calorim. 65 (2001) 451–455.
[19] Z. He, J.-I. Yamaura, Y. Ueda, W. Cheng, J. Solid State Chem. 182 (2009) 2526–2529.

[20] S. Denis, E. Baudrin, F. Orsini, G. Ouvrard, M. Touboul, J.-M. Tarascon, J. Power Sources 81–82 (1999) 79–84.
[21] E. Baudrin, S. Laruelle, S. Denis, M. Touboul, J.-M. Tarascon, Solid State Ionics 123 (1999) 139–153.
[22] A.C. Larson, R.B. Von Dreee, General Structure Analysis System (GSAS), Los Alamos National Laboratory Report LAUR 86-748, 1994.
[23] E.E. Sauerbrei, R. Faggiani, C. Calvo, Acta Cryst. B 30 (1974) 2907–2909.
[24] J.T.S. Irvine, D.C. Sinclair, A.R. West, Adv. Mater. 2 (1990) 132–138.
[25] J.C. Bernier, P. Poix, A. Michel, Bull. Soc. Chim. Fr. 1963 (1963) 1724–1728.
[26] D.B. Rogers, R.J. Arnott, A. Wold, J.B. Goodenough, J. Phys. Chem. Solids 24 (1963) 347–360.
[27] M. Nohair, D. Aymes, P. Perriat, B. Gillot, Vib. Spectrosc. 9 (1995) 181–190.